Metallophysics and Advanced Technologies
Металофіз. новітні технол.
Metallofiz. Noveishie Tekhnol.
2023, vol. 45, No. 6, pp. 757–771
Reprints available directly from the publisher

PACS numbers: 61.05.cp, 61.72.up, 65.60.+a, 68.37.Hk, 68.37.Ps, 68.55.Ln, 82.80.Pv

Aluminium Ion Implantation in Stainless Steel

V. Honcharov*, V. Zazhigalov*, and M. Honcharova**

**Institute for Sorption and Problems of Endoecology, N.A.S. of Ukraine,*
13, General Naumov Str.,
UA-03164 Kyiv, Ukraine
***Kharkiv I. P. Kotlyarevsky National University of Arts,*
11/13, Maidan Konstytutsii,
UA-61003 Kharkiv, Ukraine

As established, the implantation of aluminium in a stream of nitrogen ions on the stainless-steel surface leads to a partial recrystallization ('ferritization', inoculation with defect formation) of the carrier matrix. The SEM shows the formation of aluminium coating with thickness up to 100 nm on the carrying surface as a result of implantation. The results of XPS surface study demonstrate that this surface layer contains of the x-ray amorphous aluminium nitride, oxide and oxynitride compounds. The oxidation of composite (implant) leads to the destruction of nitrogen-containing compounds, and alumina become the base surface-layer compound. Both the specific surface area and the mechanical strength of the surface layer increase significantly after implantation and oxidation of implant as well as growth of the implantation dose too. The changes of the surface structure and morphology as well as formation of chemical compounds on the carrying agent influence on the thermal-physical characteristics (namely, increase of surface temperature and air near-surface temperature is observed) in comparison with the untreated sample.

Key words: morphology, ionic implantation, phase composition, mechanical strength.

Corresponding author: Vitaliy Viktorovych Honcharov
E-mail: milostiprosim@i.ua

Institute for Sorption and Problems of Endoecology, N.A.S. of Ukraine,
13 General Naumov Str.,
UA-03164 Kyiv, Ukraine

Citation: V. Honcharov, V. Zazhigalov, and M. Honcharova, Aluminium Ion Implantation in Stainless Steel, *Metallofiz. Noveishie Tekhnol.*, **45**, No. 6: 757–771 (2023), DOI: 10.15407/mfint.45.06.0757

Встановлено, що імплантація Алюмінію в потоці йонів Нітроґену на поверхню неіржавійної криці приводить до часткової рекристалізації («феритизації», інокуляції з утворенням дефектів) несної матриці. СЕМ показала утворення алюмінійового покриття товщиною до 100 нм на поверхні носія в результаті імплантації. Результати РФЕС-дослідження поверхні показали, що цей поверхневий шар містить рентґеноаморфні нітридні, оксидні й оксинітридні сполуки Алюмінію. Окиснення композиту (імплантату) приводить до руйнування нітроґенвмісних сполук, і оксид Алюмінію стає базовим поверхневим шаром. Питома поверхня та механічна міцність поверхневого шару значно зростають після імплантації й окиснення імплантату та підвищення дози імплантації. Зміни структури та морфології поверхні й утворення хемічних сполук на носії впливають на теплофізичні характеристики (підвищуються температура поверхні та приповерхнева температура повітря) порівняно з необробленим зразком.

Ключові слова: морфологія, йонна імплантація, фазовий склад, механічна міцність.

(Received November 9, 2022; in final version, February 28, 2023)

1. INTRODUCTION

Aluminium is widely used as a modifier of the different materials with a purpose to improve a whole range of their characteristics. In particular, presence of aluminium-based compounds in the metals and alloys leads to changes in their mechanical strength, heat resistance, electrical and thermal conductivity [1–4]. Formation of coatings containing these compounds permits to obtain thermal insulation, barrier, and catalytic layers [5–8]. Thus, the application prospects of the use of obtained alloys as the materials for the big spectrum of chemical, thermal, gas and petrochemical equipment opens.

The important investigation problem is the technology of aluminium insertion into the materials and preparation of compounds based on it. The existing methods of aluminium introduction have a number of advantages and disadvantages, which determine the choice of synthesis ways depending on the purpose of the prepared target materials [5, 6, 9]. The ion implantation is method deprived of the most of disadvantages [10–14] and this technology is the perspective for obtaining of aluminium compounds in the surface layer of metals (supports) due to their bombardment by ion beam.

The stainless steel is most perspective material for the ion implantation and it is widely used in different industries as a base for the preparation of heating elements, working parts of the equipment, carriers for catalysts, *etc.* [15–18].

In view of the above, in this work, foil of the steel 12Cr18Ni10Ti [19] was used as an initial sample (support), and the aluminium ions

were implanted in it. The physical, chemical, and thermophysical properties of the obtained composites were studied.

2. EXPERIMENTAL TECHNIQUE

The technique of composites synthesis (low-temperature ion implantation method) was detail described in the papers [20–22]. The samples were prepared on the base of foil from stainless steel 12Cr18Ni10Ti with the thick equal to 0.1 mm. The amount of implanted aluminium and nitrogen (working atmosphere) in the ions' flow were controlled by the parameters of implantation process (by the ion current strength and the ions energy) and in result was $2.5 \cdot 10^{17}$ and $5 \cdot 10^{17}$ ion/cm^2 of aluminium ions implanted, which corresponds to penetration of target ions into the depth on tens nanometres order. The part of the samples after implantation was oxidized at temperature of about 600 °C in air.

The obtained samples were examined using small-angle x-ray scattering at an angle $\beta = 270–360°$ on the device 2D X-ray Rigaku (Dmax rapid), which used for the study of thin films (XRD of thin films). Investigations of the samples by scanning electron microscopy (SEM) were realized on the device Hitachi S-400 at 5 kV with energy dispersive spectrometer Philips Cm 200 (Fritz Haber Institute, Berlin, Germany). Study of the samples surface using visible microscopy was carried out on microscope MIM-7, additionally equipped with digital camera Kodak EasyShare C1013 under degree of magnitude 1:1500. The specific surface area of the samples was determined on ASAP 2020 (Micromeritics Instr. Corp.) by krypton adsorption. The morphology of the samples surface was studied by atomic force microscopy (AFM) on Nanoscope Multi Mode V.

The assessment of mechanical strength of the modified surface layer was carried out by sclerometric method according to GOST 21318-75.

The samples surface was study by x-ray photoelectron spectroscopy (XPS) in ultrahigh vacuum ($1 \cdot 10^{-7}$ Pa) with a spectrometer equipped by semi-sphere analyser (SES R 4000, Gammadata Scienta) and calibrated according to ISO 15472:2001 (magnesium anode with energy of K_α-line 1253.6 eV). Spectrums were calibrated on a line relative to the line of C1*s*-electron with binding energy 285 eV. An effective depth of analysis calculated for a carbon matrix was of 3–5 nm.

In the laboratory setup with the ceramic base of standard hot plate, thermophysical properties of synthesized nanocomposites were explored according to [23].

3. RESULTS AND DISCUSSION

The results of the synthesized samples surface study by the method of

x-ray phase analysis of thin films [21, 22] show the presence in the surface layer of implants the structures which can be identified as phase of austenite, the peaks from planes (111), (220) and (200), which are correspond by the material of the carrier (austenitic steel). It is necessary to note, that the same fact was noted in the works [24, 25], but for the samples prepared under other modes of metal ions deposition and other metals.

The absence of the reflexes from implanted metal or its compounds can be connected with their amorphous state or the very low concentration in the surface layer (less appropriate hypothesis). In the same time, the changes of the relative intensity of peaks at the angles 2θ close to 44°, 51° and 74° can testify the effect of the stainless steel surface etching in this implantation process. The intensity of reflex from the plane (220) increases and the peak towards (200) appears can indicate about 'exposure' of bulk matrix, for which they are, in fact, characteristic.

The detailed analysis of the obtained x-ray spectra presented in Fig. 1 shows the more profound changes and difference of the surface structures of original carrier (stainless steel) and synthesized by aluminium implantation samples. The displacement of all three reflexes (111), (200) and (220) towards big angles shows that during aluminium implantation quantitative ratio of the phases austenite and ferrite changes in the direction of the ferrite concentration increasing. The same is shown for a reflex at 2θ close to 44° in corrosion-resistant steel that is nitrogen-alloyed [26] and for a reflex at 2θ close to 51° in electrospray-treated steel [27]. The difference in 2θ angle values for ferrite and austenite is less than 1 degree in these cases. As known according to the standards, the content of ferrite in initial stainless steel is less than 10%, which may complicate the identification of this phase on surface. This fact is agreeing well with the literature data [28]: ac-

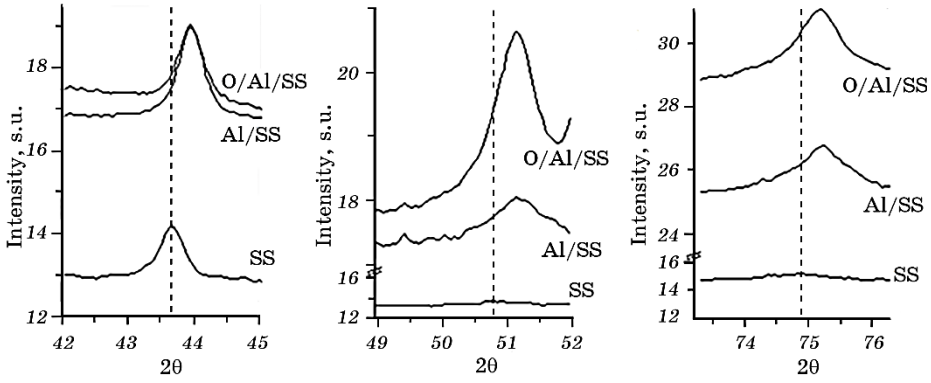

Fig. 1. The detailed diffractograms of the samples.

cording to which, aluminium is a ferritisator for alloyed steel like 12Cr18Ni10Ti, similar to Titanium, Niobium, *etc*. It is known also [29] that nitrogen is an inoculant, which can initiate the formation of nitride compounds (in particular with aluminium or titanium) and grinding of the substrate structure. As results, a decrease of the crystal lattice parameters and the shift of reflexes in the direction of large angles in diffractograms can be observed. In same time, the narrowing of these peaks for the implanted samples (Fig. 1), demonstrates an increase in 'crystallinity' or the degree of surface ordering in comparison with the untreated (initial) carrier.

The obtained results permit to propose that the implantation of aluminium and nitrogen into a stainless steel carrier leads to recrystallization of the surface layer, and this process intensifies during sample oxidation. This effect can be connected with the redistribution of the substrate internal energy caused by the introduction of high-energy particles with energy of about 30 keV and the formation of chemical compounds in the surface layer.

The methods of optical microscopy (Fig. 2) and SEM with the shooting mode of elastically reflected electrons (Fig. 3) were used to study the state of the composites surface. The microphotographs of the samples presented below show to smoothing of surface irregularities on height as a result of implantation of aluminium and nitrogen ions. It is

Fig. 2. Surface microphotographs: *a*—SS, *b*—Al/SS, implantation dose $2.5 \cdot 10^{17}$ ion/cm^2, *c*—Al/SS, implantation dose $5 \cdot 10^{17}$ ion/cm^2. Magnification ×1,500.

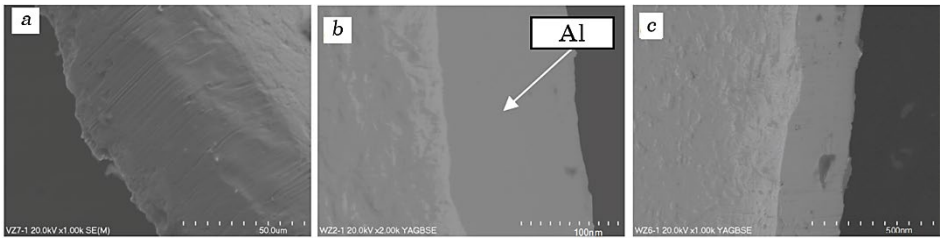

Fig. 3. Microphotographs (SEM) of the cross-section of the samples: (*a*) SS, (*b*) Al/SS, (*c*) O/Al/SS.

necessary to note that the relief smoothing is observed at different implantation doses (Fig. 2, *b*, and *c*). The data presented in Fig. 3, *b* (cross section) demonstrates that, along with the implantation, there is proceeding formation of a coating with a thickness of about 100 nm too.

The presence of aluminium in this coating is confirmed by the spectrogram (Fig. 4, *b*), which was obtained in face of the implants and demonstrates in addition to the peaks from the carrier elements (Fe, Cr, Ni, Ti, C) weak intensity signal from the Al*K*-line which indicates the low content of this component on carrier surface.

During the oxidation of composite with implant layer, the coating thickness increases to approximately 200 nm (Fig. 3, *c*). This indicates that the surface microgeometry is influenced not only by the number of implanted ions (implantation dose), but also the subsequent treatment (oxidation), and this fact should be taken into account when the implants will be using as heating elements, catalysts, *etc*.

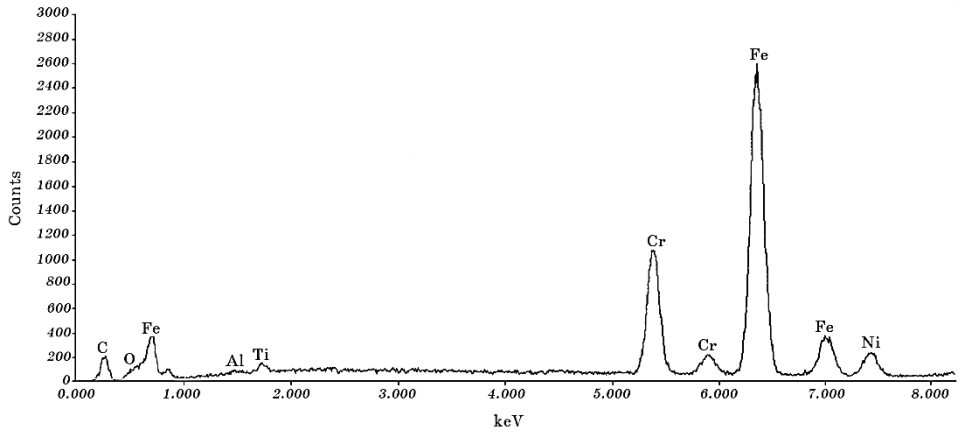

Fig. 4. Results of the surface composition analysis of the sample Al/SS on the energy dispersive spectrometer.

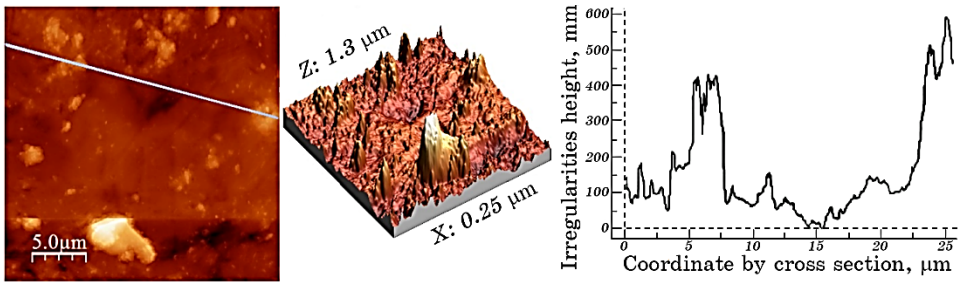

Fig. 5. AFM microphotograph (*a*) and 3D view (*b*) of the carrier surface (SS). Profile (*c*) along the line of the cross section shown in Fig. 6, *a*.

For a more detailed study of the sample surface, the AFM method was used (Fig. 5). The obtained results confirmed the data of optical microscopy and SEM on the smoothing of the sample topography after implantation and revealed important regularities of the prepared composites morphology.

As can be seen in Figs. 2, *a*, 3, *a* and 5, *b*, the surface of the untreated carrier is significantly heterogeneous. The local character of heterogeneity is clearly demonstrated by the cross section profile (Fig. 5, *c*) along the line determined in Fig. 5, *a*, in which the individual peaks with a height of almost 600 nm and large cavern are noticeable.

The implantation of aluminium and nitrogen leads to the smoothing of the surface microrelief that is proved by the data in Fig. 6 and Table 1 and is in good accordance with the data reported above. It is evident that the surface of the support after implantation becomes more uniform. It is proved by the similar dimension in the value height of the peaks (Fig. 6, *c*) and much smaller difference between the maximum and average height of the surface (Table 1) in comparison to the initial medium.

The oxidation of the composite with implanted Al and N leads to an appearance of the new narrow and shallow peaks (Fig. 7, *c*) in comparison to the Al/NS composite. In the same time, the surface inhomogeneity of the sample increases. So, in this case, the formation of secondary

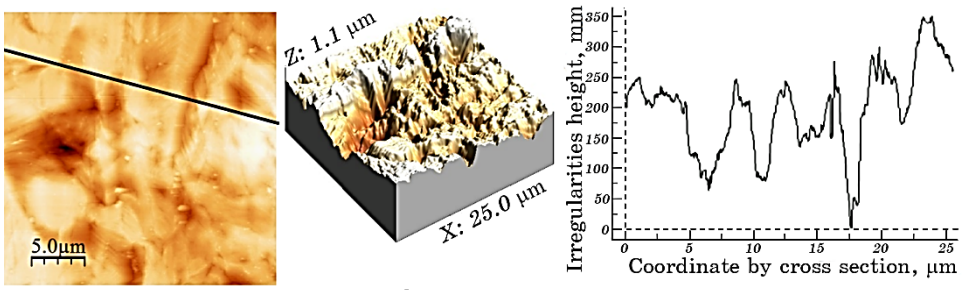

Fig. 6. AFM microphotograph (*a*) and 3D view (*b*) of the implant surface with aluminium (Al/SS). The profile along the line of the cross section shown in Fig. 7, *a*–*c*.

TABLE 1. Characteristics of sample surface microgeometry.

Sample	SS	Al/SS	O/Al/SS
Maximum height of irregularities, nm	590.9	342.4	504.0
Average height of irregularities, nm	158.8	188.9	267.3
Average surface roughness, nm	139.8	68.1	118.3
Specific surface area, cm^2/g	13.9	18.5	38.7

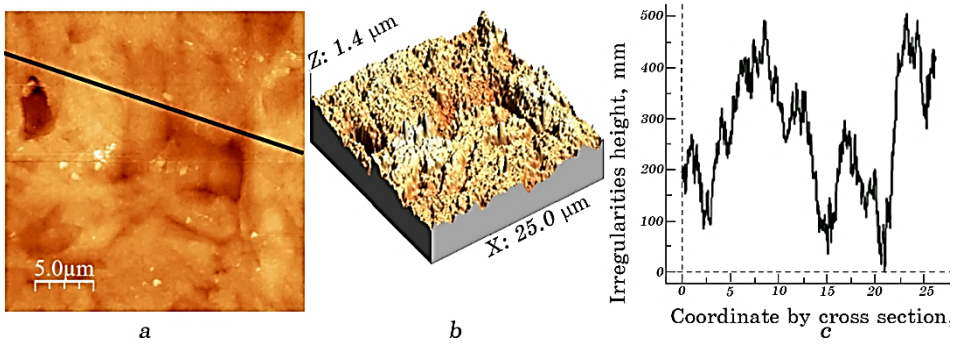

Fig. 7. AFM microphotograph (*a*) and 3D view (*b*) of the oxidized implant with aluminium (O/Al/SS). The profile along the line of the cross section shown in Fig. 8, *a*–*c*.

surface heterogeneity, which may be related to the appearance of pores because of the surface layer oxidation, can be proposed. As result, the implant oxidized by air has the more developed surface. A higher value of the specific surface area of the treated samples opens up the prospect of their application in catalysis as catalyst carriers.

In order to find out the state of the elements forming the surface layer of the treated samples the XPS method was applied. The overview of the XPS spectrum of the Al/SS composite is shown in Fig. 8, *a*. In addition to Al and N introduced by ion implantation, the presence of Fe, Ni, Ti included in the carrier (steel 12X18H10T) and O and C, which may be exist in the source material and can be sorbed from the environment (air, water, vacuum oil vapour, lubricants, *etc.*), was established. The detail study of the XPS spectra of individual elements presented below.

The decomposition of the O1*s*-electron spectrum (Fig. 8, *b*) shows the presence of five peaks for the implanted composite. Any problems with identification of four of them exists: they belong to oxygen of the crystal lattice (B), oxygen of carbonate (C) and hydroxyl groups (D), and the peak with the highest value of electrons binding energy (E) is the adsorbed oxygen on the composite surface (Fig. 8, *b*).

The first peaks of oxygen (A) characterized by the lowest value of BE of O1*s*-electrons (E_b = 527.6 eV), which can be connected with the additional transfer of electron density from the elements of the composites to oxygen. The analysis of the spectrum of N1*s*-electrons (Fig. 8, *c*) can provides additional information connected with this fact. In this spectrum the peak with binding energy value above 400 eV, which, according to the literature [30], belongs to the NO groups with significant electron density transfer from nitrogen to oxygen is observed. As the result of this effect, the peak with a low binding energy in the spectrum of O1*s*-electrons appears. The two other peaks in the spectrum of

N1*s*-electrons are associated with the formation of implanted metal nitrides and the presence of elemental nitrogen in the surface layer of the samples.

After oxidation of the sample, the changes occur both in the O1*s*-electron spectrum and in the N1*s*-electron spectrum (Fig. 8, *d*, and *e*). The spectrum of the last element practically disappears and only one component can be distinguished in it (Fig. 8, *e*), which refers to the elemental nitrogen, obviously incorporated into the carrier matrix, which oxidation occurs with low rate. In the O1*s*-electron spectrum (Fig. 8, *d*), three components, which refer to the lattice oxygen of the implanted metal oxide, carbonate groups C=O and chemisorbed water, remain (the reflex from later has the maximum intensity among them).

The analysis of O1*s*-electron and N1*s*-electron spectra permits to suggest that after implantation of aluminium and nitrogen on stainless steel foil in the surface layer of composites the formation of aluminium nitride, oxide and oxynitride compounds proceeds. After oxidation, the composite with implants lose a large amount of nitrogen, with alumina formation and this elemental rearrangement leads to texturing changes shown by SEM and AFM data, which are accompanied by an increase of SSA of the sample.

The results of the study of the spectrum of Al2*s*-electrons (Fig. 8, *f*) have good accordance with presented above based on analysis of O1*s*- and N1*s*-electron spectra. Three peaks can be distinguished in this spectrum of Al2*s*-electrons. The first one with $E_b = 116.3$ eV, according to the literature data [30, 31], refers to metallic aluminium (relative intensity of 8%). The second peak ($E_b = 119.1$ eV) characterizes the formation of aluminium nitride and its relative intensity is 20%. For the third peak, a high value of binding energy of the Al2*s*-electron ($E_b = 122.4$ eV) was found, which characterizes a significant transfer of electron density from metal to another element(s). Such values are usually observed for aluminium compounds with ligands that have a significant negative charge (Cl, F). In our case (due to the absence of fluorine or chlorine in the sample), this may be due to the formation of NO groups (see above), which provokes an additional electron density transfer from aluminium. In general, the data on the XP-spectra of O1*s*-, N1*s*- and Al2*s*-electrons are each other accordance and indicate the presence of oxide, nitride and oxynitride aluminium compounds in the surface of synthesized composites.

The oxidation of the implant by air oxygen leads to a significant change in the spectrum of Al2*s*-electrons (Fig. 8, *g*). There is only one peak in the spectrum with $E_b = 118.9$ eV, which characterizes the presence of Al in its oxide compounds. This fact agrees well enough with the changes in the spectrum of O1*s*-electrons (Fig. 8, *d*), which shows the presence of oxygen in metal oxides, as well as with the spectrum of N1*s*-electrons (Fig. 8, *e*), in which only elemental nitrogen is present.

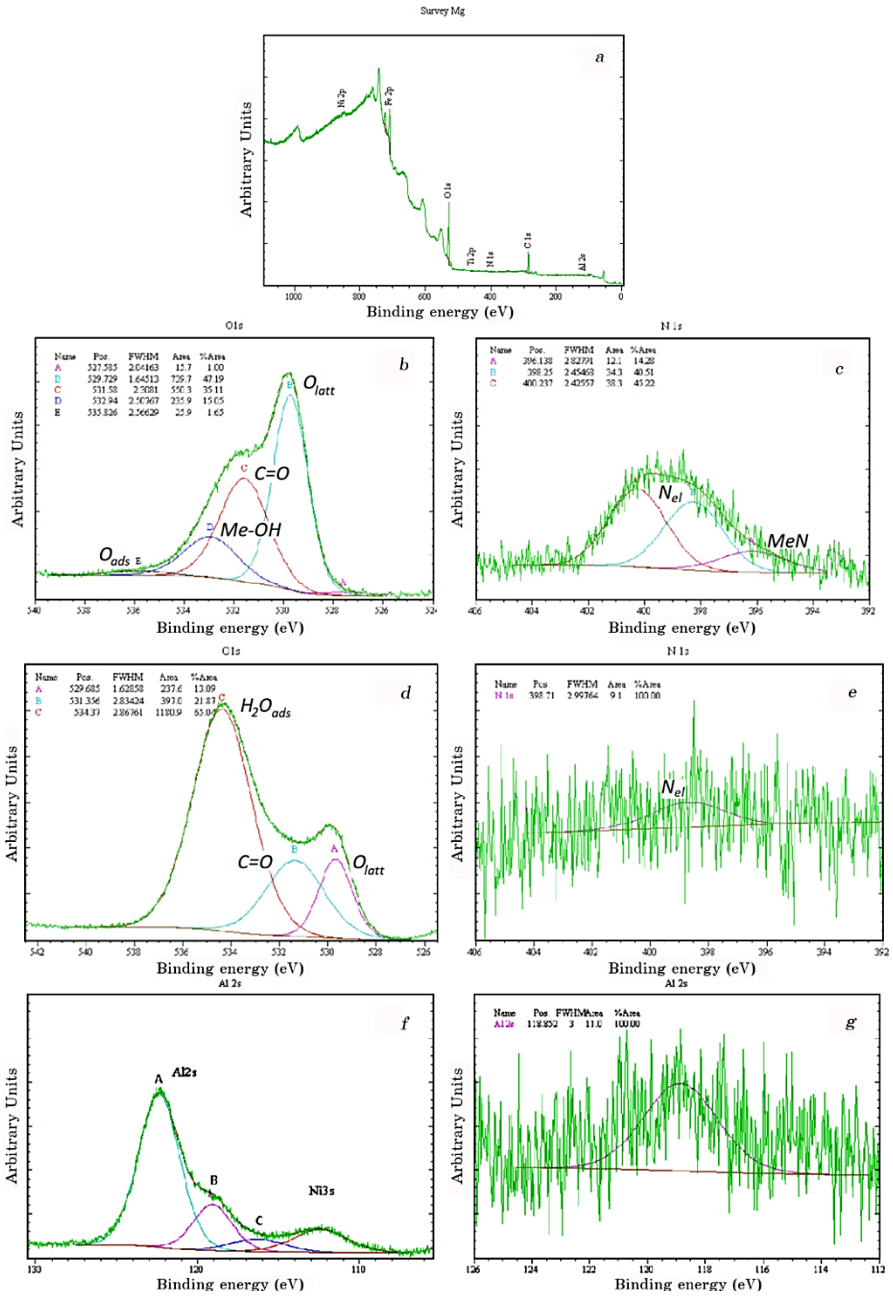

Fig. 8. Overview of the XPS spectrum of the Al/SS composite (*a*), O1*s*-electron spectrum of the Al/SS (*b*), N1*s*-electron spectrum of the Al/SS (*c*), O1*s*-electron spectrum of the O/Al/SS (*d*), N1*s*-electron spectrum of the O/Al/SS (*e*), Al2*s*-electron spectrum of the Al/SS (*f*), Al2*s*-electron spectrum of the O/Al/SS *(g)*.

The resistance of the synthesized composites to mechanical stresses was tested in sclerometry studies implemented according to the method described in [32].

The smooth scratch edges on the composite samples (Fig. 9, *b*, *c*), without visible tears, which are observed for composites with different doses of implantation testify the high plasticity of the surface layer in comparison to the original carrier (Fig. 9, *a*). The observed deformation character and the reduction of the groove thickness demonstrate an increase in the strength and hardness of the implant surface compared to the original carrier. The data obtained by sclerometry study demonstrate the high adhesive strength of the supported implant layer, the formation of which on the carrier was shown above and it is in good accordance with the mechanical strength calculations realized according to the method [32] (Table 2). The observed hardening effect in composite surface can be due to defect formation in the carrier matrix under the embedding in the support material of nitrogen and aluminium ions, which agrees with the data of the XRD of thin films and XPS study. In addition, the cascade of perturbation caused by impurity particles can lead not only to the concentration of the Schottky and Frenkel defects, but also to the redistribution of stresses, up to the output of energy waves on the surface, which is reflected in the form of its topography and is confirmed by optical microscopy, SEM and AFM results.

To determine the possibility of application of the synthesized composites as the elements of heaters, gas burners, catalysts, *etc.*, their thermophysical characteristics were studied. The comparison of ther-

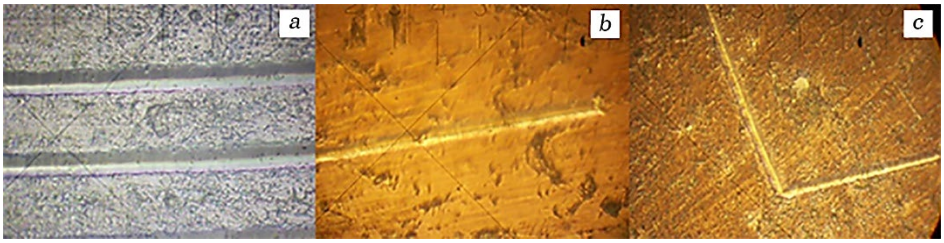

Fig. 9. Microphotographs of the carrier surface (SS) (*a*), and Al/SS samples with implantation doses of $2.5 \cdot 10^{17}$ ion/cm^2 (*b*) and $5 \cdot 10^{17}$ ion/cm^2 (*c*) after scratching. Magnification ×200.

TABLE 2. Characteristics of mechanical strength of the samples surface.

Sample	SS	Al/SS	O/Al/SS
Implantation dose, ion/cm^2	—	$2.5 \cdot 10^{17}$	$5 \cdot 10^{17}$
Mechanical strength, GPa	1.7	3.4	5.7

mal properties of the implants and the initial medium was carried out according to the technique [23] in a laboratory flow-through facility at an air flow rate of 600 l/hour and by passing through materials (support and composites) an electric current of different power.

The obtained results show (Fig. 10, *a*) that the implants (composites) have a higher value of heat transfer coefficient from the sample to the air than initial carrier does. This can be connected with the difference in samples surface area, their surface shape and temperature.

Since the differences in area and microgeometry of the samples surface were shown above by BET, AFM, SEM methods, we realized the temperature studies. The obtained presented in Figs. 10, *a* and *b*. This data show that, firstly, the air temperature near to the implants surface is approximately 25–35°C (in dependence from electric power) higher than the air temperature near the untreated support surface.

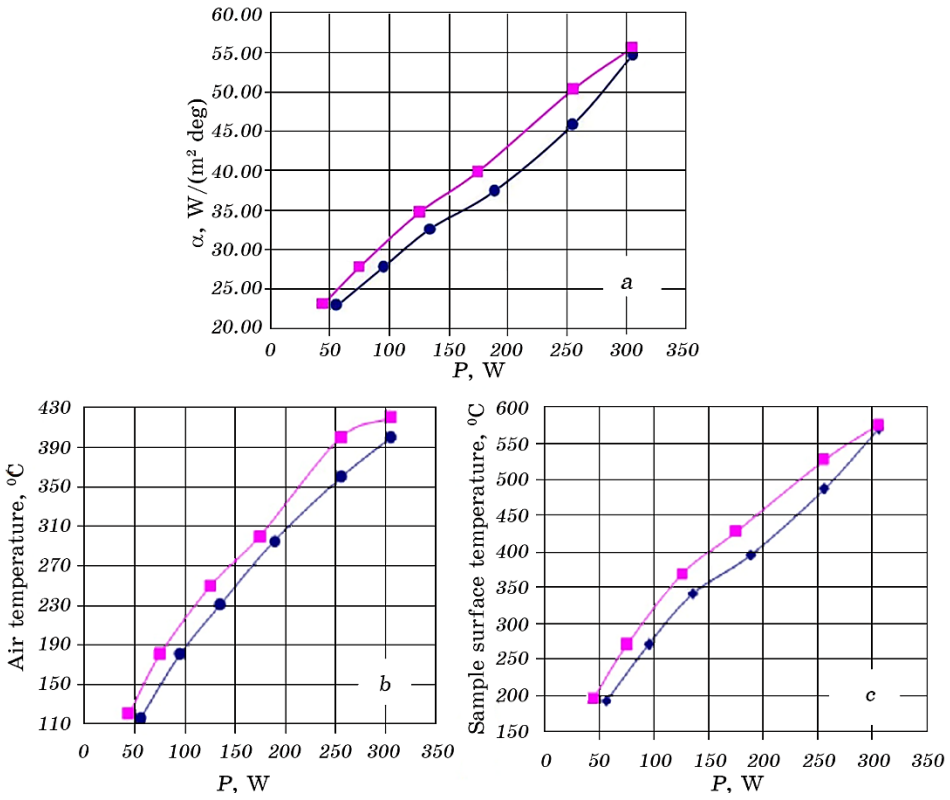

Fig. 10. The dependence of the heat transfer coefficient (*a*), the air temperature above the burner (*b*) and the surface temperature (*c*) on the power consumed for heating for the samples: ●—original carrier (SS); ■—Al/SS composite, with an implantation dose of $5 \cdot 10^{17}$ ions/cm^2.

Secondly, the surface temperature of implant is average on 30–40°C higher than the temperature of the initial support surface.

The reason of the difference in the temperature indices above for initial sample and composite can be the presence (according to the XPS results) of aluminium, oxygen and nitrogen-based aluminium compounds (oxides, nitrides and oxynitrides) in the implant surface layer, which impairs the electrical and thermal conductivity in the layer and as a result can lead to the local overheating of surface. In addition, the existence of coating layer in support surface (detected by SEM, cross section; Fig. 3) can, in its turn, act as a thermal barrier preventing the dissipation of heat deep into the material and promote its concentration on the surface.

4. CONCLUSION

The obtained results shown that the implantation of aluminium in a stream of nitrogen ions on stainless steel surface leads to a complex effect on the initial material properties.

It is shown that the introduction of Al and N ions into the carrier matrix accompanied by its partial recrystallization ('ferritization', inoculation with defect formation). The partial introduction of implanted aluminium and nitrogen ions into stainless steel leads to the changes of the support near-surface layer structure.

The formation of aluminium coating with thickness up to 100 nm on carrier surface as result of implantation was observed. It was established that this surface layer contains the x-ray amorphous aluminium nitride, oxide and oxynitride compounds. The oxidation of composite (implant) leads to the destruction of nitrogen containing compounds and alumina become the base surface layer compound.

It was established that the specific surface area and the mechanical strength of the surface layer increase significantly after implantation and oxidation of implant and the growth of the implantation dose too.

It is established that the structural and morphological changes as well as formation of chemical compounds on the carrier increase the thermal-physical characteristics of the implants in comparison with the properties of the untreated sample.

Therefore, the practical usefulness of the synthesized composites can be connected with their application as support for catalysts synthesis, elements of heating devices and other construction materials of chemical, oil, and gas industry.

REFERENCES

1. H. Kang, C. I. Garcia, K. Chin, and A. J. Deardo, *ISIJ Int.*, **47**, No. 3: 486

(2007).
2. *Novyye Materialy* [New Materials] (Ed. Yu. S. Karabasov) (Moskva: MISiS: 2002) (in Russian).
3. Y. Adraider, S. N. B. Hodgson, M. C. Sharp, Z. Y. Zhang, F. Nabhani, A. Al-Waidh, and Y. X. Pang, *JECS*, **32**, No. 16: 4229 (2012).
4. S. El Hajjaji, M. El Alaoui, P. Simon, A. Guenbour, A. Ben Bachir, E. Puech-Costes, M.-T. Maurette, and L. Aries, *STAM*, **6**, No. 5: 519 (2005).
5. T. Novakovic, N. Radic, B. Grbic, V. Dondur, M. Mitric, D. Randjelovic, D. Stoychev, and P. Stefanov, *Applied Surface Science*, **255**, No. 5: 3049 (2008).
6. P. Stefanov, D. Stoychev, A. Aleksandrova, D. Nicolova, G. Atanasova, and Ts. Marinova, *Applied Surface Science*, **235**, Nos. 1–2: 80 (2004).
7. M. P. Vorob'eva, A. A. Greish, A. V. Ivanov, and L. M. Kustov, *Appl. Catalysis A: General*, **199**, No. 2: 257 (2000).
8. K. Spencer, D. M. Fabijanic, and M.-X. Zhang, *Surface and Coatings Technology*, **206**, Nos. 14–15: 3275 (2012).
9. N. I. Radishevskaya and V. I. Vereshchagin, *Butlerovskie Soobshcheniya*, **25**, No. 8: 75 (2011) (in Russian).
10. B. A. Kalin, *Fizika i Khimiya Obrabotki Materialov*, **4**, No. 5: 5 (2001) (in Russian).
11. A. A. Cherny, S. V. Maschenko, V. V. Honcharov, and V. A. Zazhigalov, *Nanoplasmonics, Nano-Optics, Nanocomposites, and Surface Studies. Springer Proceedings in Physics* (Cham: Springer: 2015), vol.**167**, p. 203.
12. L. B. Begrambekov, *Modifikatsiya Poverkhnosti Tverdykh Tel pri Ionnom i Plazmennom Vozdeystvii* [Surface Modification of Solids at the Ionic and Plasma Actions] (Moskva: MIFI: 2001) (in Russian).
13. M. G. Bannikov, J. A. Chattha, V. N. Zlobin, I. P. Vasilev, J. A. Cherkasov, and P. N. Gawrilenko, *Proc. of the 7th International Symposium on Advanced Materials (Sep. 17–21, 2001)* (Islamabad, Pakistan: International Atomic Energy Agency (IAEA): 2001), p. 341.
14. V. Honcharov and V. Zazhigalov, *Int. J. Biosen Bioelectron*, **4**, No. 3: 98 (2018).
15. I. N. Golikov, A. P. Gulyayev, A. S. Kaplan, and O. I. Putimtseva, *Stali Vysokolegirovannyye i Splavy Korrozionnostoykie, Zharostoykie i Zharoprochnyye. Marki* [High-Alloy Steels and Alloys, Which Are Corrosion-Resistant, Heat-Resistant and Heat-Resistant. Grades] (GOST 5632-72) (Moskva: Gosudarstvennyy Komitet Standartov Soveta Ministrov SSSR: 1975) (in Russian).
16. M. Nomura, B. Meester, J. Schoonman, F. Kapteijn, and J. A. Moulijn, *Separation and Purification Technology*, **32**, Nos. 1–2: 387 (2003).
17. D. Truyen, M. Courty, P. Alphonse, and F. Ansart, *Thin Solid Films*, **495**, Nos. 1–2: 257 (2006).
18. T. Giornelli, A. Lofberg, L. Guillou, S. Paul, V. Le Courtois, and E. Bordes-Richard, *Catalysis Today*, **128**, Nos. 3–4: 201 (2007).
19. *Lenta Kholodnokatanaya iz Korrozionnostoykoy i Zharostoykoy Stali. Tekhnicheskie Usloviya* [Cold-Rolled Strips of Corrosion-Resistant and Heat-Resistant Steel. Specifications] (GOST 4986-79) (Moskva: Gosudarstvennyy Komitet Standartov Soveta Ministrov SSSR: 1980) (in Russian).
20. A. V. Katruha, V. V. Goncharov, and V. O. Zazhigalov, *Int. J. Energy for a Clean Environment*, **17**, Nos. 2–4: 133 (2016).
21. V. Honcharov, V. Zazhigalov, Z. Sawlowicz, R. Socha, and J. Gurgol, *Nano-*

physics, Nanomaterials, Interface Studies, and Applications. NANO 2016. Springer Proceedings in Physics (Cham: Springer: 2017), vol. **195**, p. 355 (2017).

22. S. Kryvoruchko, A. Kryvoruchko, V. V. Honcharov, and V. O. Zazhigalov, *Ukrainian Journal of Physics*, **67**, No. 4: 292 (2022).
23. V. V. Goncharov, A. O. Klimash, V. O. Zazhigalov, and V. M. Orlik, *Fizika i Khimiya Tverdoho Tila*, **12**, No. 36: 762 (2011) (in Ukrainian).
24. J. Dudognon, M. Vayer, A. Pineau, and R. Erre, *Surface & Coating Technology*, **202**, No. 20: 5048 (2008).
25. Y. D. Park, I. S. Maroef, A. Landau, and D. L. Olson, *Welding J.*, **81**, No. 2: 27 (2002).
26. S. O. Muradyan, *Struktura i Svoystva Liteynoy Korrozionnostoykoy Stali, Legirovannoy Azotom* [Structure and Properties of Nitrogen-Alloyed Corrosion-Resistant Steel] (Thesis of Disser. for PhD) (Moskva: Baikov Institute of Metallurgy and Materials Science, Russian Academy of Sciences: 2015) (in Russian).
27. A. I. Mihaylyuk and G. F. Volodina, *Ehlektronnaya Obrabotka Materialov*, **6**: 53 (2010) (in Russian).
28. O. B. Perevalova, *Mikrostruktura Legirovannykh Staley* [Microstructure of Alloyed Steels] (Tomsk: TGASU: 2011) (in Russian).
29. Ya. E. Gol'dshtein and V. G. Mizin, *Inokulirovanie Zhelezouglerodistykh Rasplavov* [Inoculation of Iron–Carbon Melts] (Moskva: Metallurgiya: 1993) (in Russian).
30. *XPS Data Base. THERMO Electron France Les Mimosas, 16 Av du Quebec SILIC 765, 91963 COURTABOEUF CEDEX*: http://www.lasurface.com
31. V. I. Nefedov, *Rentgenoehlektronnaya Spektroskopiya Khimicheskikh Soyedineniy* [X-Ray Electron Spectroscopy of Chemical Compounds] (Moskva: Khimiya: 1984) (in Russian).
32. *Izmerenie Mikrotverdosti Tsarapaniem Almaznymi Nakonechnikami* [Measurement of Microhardness by Scratching with Diamond Instruments] (GOST 21318-75) (Moskva: Gosudarstvennyy Komitet Standartov Soveta Ministrov SSSR: 1975) (in Russian).